

Multilabel Classification with Label Correlations and Missing Labels

Wei Bi James T. Kwok

Department of Computer Science and Engineering
 Hong Kong University of Science and Technology
 Hong Kong
 {weibi, jamesk}@cse.ust.hk

Abstract

Many real-world applications involve multilabel classification, in which the labels can have strong interdependencies and some of them may even be missing. Existing multilabel algorithms are unable to handle both issues simultaneously. In this paper, we propose a probabilistic model that can automatically learn and exploit multilabel correlations. By integrating out the missing information, it also provides a disciplined approach to the handling of missing labels. The inference procedure is simple, and the optimization subproblems are convex. Experiments on a number of real-world data sets with both complete and missing labels demonstrate that the proposed algorithm can consistently outperform state-of-the-art multilabel classification algorithms.

Introduction

In multilabel classification, a sample may be assigned multiple labels. This is different from multiclass classification, in which one and only one label can be assigned to each sample. Many real-world applications involve multilabel classification. Examples include text categorization, image annotation, and gene function analysis (Zhang and Zhou 2013).

A popular baseline for multilabel classification is binary relevance (BR) (Tsoumakas, Katakis, and Vlahavas 2010), which simply treats each label as a separate binary classification problem. However, its performance can be poor when strong label dependencies exist. For example, an article on “sports” may also be labeled “entertainment”; an image annotated with “jungle” may also be tagged with “bushes”. To improve prediction performance, recent multilabel classification algorithms all try to exploit label dependencies.

One approach is to assume that the label dependencies are known a priori or can be easily estimated. For example, the classifier chain (CC) algorithm (Read et al. 2009) incorporates label correlations implicitly by training a chain of BR classifiers in a given sequential order, with the feature set of each BR classifier augmented by labels that have been previously trained. In the max-margin multilabel classifier (M3L) (Hariharan et al. 2010) and the method by (Pettersson and Caetano 2011), label dependencies are represented by

pairwise label correlations that are computed from the training set. However, this may be crude and inaccurate as the number of training samples associated with a label can be very few. For example, in the corel5k data set, which contains images collected from the Corel CD (Duygulu et al. 2002), 180 of its 260 labels have fewer than 50 positive samples. Similarly, in the ESP game data set, which contains images collected for the ESP collaborative image labeling task (Von Ahn and Dabbish 2004), 110 of its 268 labels have fewer than 150 positive samples. Alternatively, Zhang and Zhang (2010) used a more sophisticated Bayesian network structure learning algorithm (Koivisto and Sood 2004) to estimate the label dependencies. However, it is much more expensive and time-consuming. Recently, a number of multiple-output relationship learning algorithms have been proposed (Rai, Kumar, and Iii 2012; Zhang and Yeung 2010; Rothman, Levina, and Zhu 2010). They also aim to capture output correlations, but are usually designed for regression problems rather than multilabel classification problems.

Another approach aims to remove label dependencies by transforming the labels, such that the decorrelated labels can be learned separately. For example, Hsu et al. (2009) employed a randomized matrix for label transformation; Principal label space transformation (PLST) (Tai and Lin 2012) uses singular value decomposition (SVD) on the label matrix; Conditional principal label space transformation (CPLST) (Chen and Lin 2012) performs SVD on a matrix involving both the label matrix and input sample matrix.

Besides the presence of label correlations, another challenging problem in multilabel classification is that we may not have access to all the true labels of each training sample. For example, many image annotation tasks use crowdsourcing platforms to collect labels. For each image, the workers may only provide a small, incomplete set of answers to the queried labels.

Existing algorithms are often incapable of handling both label correlations and missing labels. To alleviate this problem, a simple solution is to discard all samples with missing labels, though at the expense of potentially losing a significant amount of label information. Another approach is to estimate the missing labels, particularly the positive ones. For example, the multilabel ranking with group lasso (ML-RGL) algorithm (Bucak, Jin, and Jain 2011) formulates multilabel classification as a bipartite ranking problem, and sets

all missing labels as negative. To detect the possibly missing positive labels, it uses group lasso (Yuan and Lin 2006) to selectively penalize the pairwise ranking errors between the two partitions. Fast image tagging (FastTag) (Chen, Zheng, and Weinberger 2013) recovers the possibly missing positive labels by assuming that the labels are uniformly corrupted. A limitation of these methods is that label correlations cannot be explicitly incorporated. Recently, Yu, Jain, and Dhillon (2014) provided an analysis for missing labels based on empirical risk minimization. However, it also does not explicitly consider label correlations.

In this paper, we propose a probabilistic model that can simultaneously capture label dependencies and handle missing labels. Unlike MLRGL and FastTag, we adopt the more general setting where both positive and negative labels can be missing (Yu, Jain, and Dhillon 2014; Xu, Jin, and Zhou 2013; Kapoor, Viswanathan, and Jain 2012; Goldberg et al. 2010). In other words, a label can be labeled as “positive”, “negative” or “missing”. Our model is motivated by the aforementioned label transformation approach which tries to decorrelate labels (Tai and Lin 2012; Chen and Lin 2012). However, instead of explicitly finding a label transform, we re-express the probabilistic model back to the original label space. It will be shown that the inference can be performed easily, and missing labels can be naturally handled by integrating them out. Experiments on a number of real-world data sets show that the proposed approach can outperform the state-of-the-art.

Notation: In the sequel, the transpose of vector/matrix is denoted by the superscript T , the trace of a matrix $\mathbf{A} = [a_{ij}]$ is denoted $\text{tr}(\mathbf{A})$, its determinant as $|\mathbf{A}|$, inverse as \mathbf{A}^{-1} , pseudo-inverse as \mathbf{A}^\dagger , Frobenius norm as $\|\mathbf{A}\|_F$, and $\|\mathbf{A}\|_1 = \sum_{ij} |a_{ij}|$. $\mathbf{A}_{(i,:)}$ (resp. $\mathbf{A}_{(:,i)}$) is the i th row (resp. column) of \mathbf{A} . Moreover, $\mathbf{0}$ is the zero vector, $\mathbf{1}$ is the vector of all ones, \mathbf{I} is the identity matrix, $\mathcal{N}(\boldsymbol{\mu}, \boldsymbol{\Sigma})$ denotes the normal distribution with mean $\boldsymbol{\mu}$ and covariance matrix $\boldsymbol{\Sigma}$.

Related Work: Label Transformation

In a multilabel classification problem, we are given training samples $\{(\mathbf{x}, \mathbf{y})\}$, where $\mathbf{x} \in \mathbb{R}^d$ is the input, and $\mathbf{y} \in \{0, 1\}^m$ is the corresponding output. The label transformation approach (Tai and Lin 2012; Chen and Lin 2012) transforms each \mathbf{y} to $\tilde{\mathbf{y}} = \mathbf{P}\mathbf{y}$, where $\mathbf{P} \in \mathbb{R}^{\tilde{m} \times m}$, such that the labels $\{\tilde{y}_i\}_{i=1}^{\tilde{m}}$ in the transformed space are uncorrelated and can be trained separately. In the following, we use a linear model (with weight $\tilde{\mathbf{w}}_i$ and bias \tilde{b}_i) as the learner. Equivalently, \tilde{y}_i is assumed to be generated as:

$$\tilde{y}_i | \mathbf{x}, \tilde{\mathbf{w}}_i, \tilde{b}_i, \tilde{\sigma}_i \sim \mathcal{N}(\tilde{\mathbf{w}}_i^T \mathbf{x} + \tilde{b}_i, \tilde{\sigma}_i^2), \quad i = 1, \dots, \tilde{m}, \quad (1)$$

where $\tilde{\sigma}_i^2$ is the noise variance. Note that the Gaussian noise is used here as the transformed labels are real-valued in general (even though the original ones are binary-valued). Equation (1) can be written in a more compact form, as

$$\tilde{\mathbf{y}} | \mathbf{x}, \tilde{\mathbf{W}}, \tilde{\mathbf{b}}, \tilde{\boldsymbol{\Omega}} \sim \mathcal{N}(\tilde{\mathbf{W}}^T \mathbf{x} + \tilde{\mathbf{b}}, \tilde{\boldsymbol{\Omega}}), \quad (2)$$

where $\tilde{\mathbf{W}} = [\tilde{\mathbf{w}}_1, \dots, \tilde{\mathbf{w}}_{\tilde{m}}]$, $\tilde{\mathbf{b}} = [\tilde{b}_1, \dots, \tilde{b}_{\tilde{m}}]^T$, and $\tilde{\boldsymbol{\Omega}} = \text{diag}(\tilde{\sigma}_1^2, \dots, \tilde{\sigma}_{\tilde{m}}^2)$. As usual, we also add a Gaussian prior

(essentially, ℓ_2 -regularizer) on $\tilde{\mathbf{w}}_i$:

$$\tilde{\mathbf{w}}_i | \tilde{\boldsymbol{\Sigma}}_i \sim \mathcal{N}(\mathbf{0}, \tilde{\boldsymbol{\Sigma}}_i), \quad (3)$$

where $\tilde{\boldsymbol{\Sigma}}_i = \text{diag}(\frac{1}{\alpha_{i,1}}, \dots, \frac{1}{\alpha_{i,d}})$. As the \tilde{m} labels are independent, the $\{\alpha_{i,d}\}_{i=1}^{\tilde{m}}$ values (for the same feature d) are also different in general. From the learned $\tilde{\mathbf{y}}$, we can back-project to the original label space and obtain

$$\mathbf{z} = \mathbf{P}^\dagger \tilde{\mathbf{y}}. \quad (4)$$

Often, this has to be rounded to get back a binary prediction.

The various label transformation methods mainly differ in how the transformation matrix \mathbf{P} is obtained. For example, in the CPLST (Chen and Lin 2012), \mathbf{P} is orthogonal and is obtained by jointly minimizing the training error $\|\mathbf{P}\mathbf{Y} - \tilde{\mathbf{W}}^T \mathbf{X}\|_F^2$ in the transformed space and the error $\|\mathbf{Y} - \mathbf{P}^\dagger \mathbf{P}\mathbf{Y}\|_F^2$ in encoding the original labels by the transformed labels.

Handling Label Correlations

Instead of explicitly finding the label transformation matrix, we consider in this section re-expressing the probabilistic model for the label transformation approach back in the original label space. This is advantageous for two reasons. (i) It can be naturally extended for missing labels (as will be seen in the next section); (ii) Prior knowledge on label and task correlations can be easily incorporated.

Model

Using (2), (4), and a change of variables $\mathbf{W} = \tilde{\mathbf{W}}\mathbf{P}^{\dagger T}$, $\mathbf{b} = \mathbf{P}^\dagger \tilde{\mathbf{b}}$, and $\boldsymbol{\Omega} = \mathbf{P}^\dagger \tilde{\boldsymbol{\Omega}} \mathbf{P}^{\dagger T}$, it is easy to show that the multilabel prediction before rounding, i.e., \mathbf{z} in (4), follows the normal distribution:

$$\mathbf{z} | \mathbf{x}, \mathbf{W}, \mathbf{b}, \boldsymbol{\Omega} \sim \mathcal{N}(\mathbf{W}^T \mathbf{x} + \mathbf{b}, \boldsymbol{\Omega}). \quad (5)$$

Here, $\boldsymbol{\Omega}$ can be seen to capture label correlation. Note that while the transformed labels \tilde{y} 's are assumed to be independent, the z_i 's can be highly correlated because of the shared matrix \mathbf{P}^\dagger in (4). Hence, $\boldsymbol{\Omega}$ is not diagonal in general. As $\boldsymbol{\Omega}$ directly encodes the label correlation, prior knowledge can be easily incorporated. For example, one can use

$$p(\boldsymbol{\Omega}) \propto \exp\left(-\frac{1}{\lambda_1} \|\boldsymbol{\Omega}^{-\frac{1}{2}}\|_F^2 - \frac{1}{\lambda_2} \|\boldsymbol{\Omega}^{-1}\|_1\right), \quad (6)$$

where $\lambda_1, \lambda_2 > 0$, to encourage sparsity and shrinkage on $\boldsymbol{\Omega}^{-1}$. Recall that $\boldsymbol{\Omega}^{-1}$ is the precision matrix, and $\boldsymbol{\Omega}_{ij}^{-1}$ measures the partial correlation between labels i and j (Lauritzen 1996). Encouraging sparsity on $\boldsymbol{\Omega}^{-1}$ thus represents the prior belief that most label pairs are conditionally independent given the other labels. Moreover, $p(\boldsymbol{\Omega})$ is expressed in terms of $\boldsymbol{\Omega}^{-1}$ instead of $\boldsymbol{\Omega}$. As will be seen, this allows the inference procedure to be computationally tractable.

To model the rounding error from \mathbf{z} to the binary prediction \mathbf{y} , we approximate this by a normal distribution for simplicity, as:

$$\mathbf{y} | \mathbf{z} \sim \mathcal{N}\left(\mathbf{z}, \frac{1}{\lambda_0} \mathbf{I}\right), \quad (7)$$

where $\lambda_0 > 0$.

Finally, the distribution of \mathbf{W} can be obtained from that of $\tilde{\mathbf{W}}$ as follows. First, we vectorize \mathbf{W}^T ,

$$\begin{aligned} \text{vec}(\mathbf{W}^T) &= [\mathbf{W}_{(1,:)}, \dots, \mathbf{W}_{(d,:)}]^T \\ &= [\tilde{\mathbf{W}}_{(1,:)} \mathbf{P}^{\dagger T}, \dots, \tilde{\mathbf{W}}_{(d,:)} \mathbf{P}^{\dagger T}]^T \\ &= \mathbf{Q} [\tilde{\mathbf{W}}_{(1,:)}, \dots, \tilde{\mathbf{W}}_{(d,:)}]^T, \end{aligned}$$

where $\mathbf{Q} = \begin{bmatrix} \mathbf{P}^\dagger & \mathbf{0} \\ & \ddots \\ \mathbf{0} & \mathbf{P}^\dagger \end{bmatrix}$. Using (3), we have

$$\text{vec}(\mathbf{W}^T) \sim \mathcal{N} \left(\mathbf{0}, \mathbf{Q} \begin{bmatrix} \text{diag}(\boldsymbol{\alpha}_1) & & \mathbf{0} \\ & \ddots & \\ \mathbf{0} & & \text{diag}(\boldsymbol{\alpha}_d) \end{bmatrix} \mathbf{Q}^T \right),$$

where $\boldsymbol{\alpha}_j = [\alpha_{1,j}, \dots, \alpha_{m,j}]^T$. In other words, the $\mathbf{W}_{(j,:)}$'s are independent, and each $\mathbf{W}_{(j,:)}$ is distributed as

$$\mathbf{W}_{(j,:)} | \boldsymbol{\Sigma}_j \sim \mathcal{N}(\mathbf{0}, \boldsymbol{\Sigma}_j), \quad j = 1, 2, \dots, d, \quad (8)$$

where $\boldsymbol{\Sigma}_j = \mathbf{P}^\dagger \text{diag}(\boldsymbol{\alpha}_j) \mathbf{P}^{\dagger T}$ captures the task correlation for feature j and is not diagonal in general. Analogous to (6), we can also impose the following prior on each $\boldsymbol{\Sigma}_j$

$$p(\boldsymbol{\Sigma}_j) \propto \exp \left(-\frac{1}{\beta_1} \|\boldsymbol{\Sigma}_j^{-\frac{1}{2}}\|_F^2 - \frac{1}{\beta_2} \|\boldsymbol{\Sigma}_j^{-1}\|_1 \right), \quad (9)$$

where $\beta_1, \beta_2 > 0$. A graphical model representation for the whole model is shown in Figure 1.

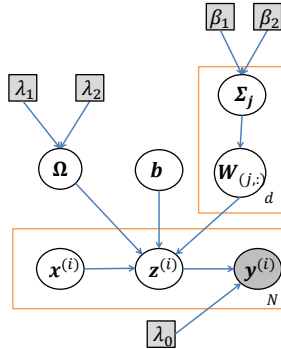


Figure 1: Graphical model representation of the proposed model.

Discussion

If $\boldsymbol{\Sigma}_1 = \boldsymbol{\Sigma}_2 = \dots = \boldsymbol{\Sigma}_d = \boldsymbol{\Sigma}$, (8) can be rewritten as

$$\mathbf{W} | \boldsymbol{\Sigma} \sim \mathcal{MN}_{d,m}(\mathbf{0}, \mathbf{I} \otimes \boldsymbol{\Sigma}), \quad (10)$$

where \otimes is the Kronecker product, and $\mathcal{MN}_{d,m}(\cdot, \cdot)$ is the $d \times m$ matrix-variate normal distribution¹ (Gupta and Nagar 2000). By

¹A random variable $\mathbf{X} \in \mathbb{R}^{m \times n}$ follows the *matrix-variate normal distribution* $\mathcal{MN}_{m,n}(\mathbf{M}, \boldsymbol{\Psi} \otimes \boldsymbol{\Sigma})$ with mean $\mathbf{M} \in \mathbb{R}^{m \times n}$ and covariance matrix $\boldsymbol{\Psi} \otimes \boldsymbol{\Sigma}$ (where $\boldsymbol{\Psi} \in \mathbb{R}^{m \times m}$ and $\boldsymbol{\Sigma} \in \mathbb{R}^{n \times n}$) if its pdf is given by $(2\pi)^{-\frac{mn}{2}} |\boldsymbol{\Psi}|^{-\frac{m}{2}} |\boldsymbol{\Sigma}|^{-\frac{n}{2}} \exp(-\frac{1}{2} \text{tr}[\boldsymbol{\Psi}^{-1}(\mathbf{X} - \mathbf{M})\boldsymbol{\Sigma}^{-1}(\mathbf{X} - \mathbf{M})^T])$.

further dropping the rounding error in (7), the proposed model reduces² to the multiple-output regression with output and task structures (MROTS) model recently proposed in (Rai, Kumar, and Iii 2012). The flexibility of modeling task correlation in a feature-specific manner can be beneficial. For example, in annotating images of different animals, it may not be appropriate to encourage features such as “long-legs” and “hairless” to share the same task correlation.

Modeling the rounding in (7) explicitly is also useful in classification problems. In (Tai and Lin 2012; Chen and Lin 2012), this rounding leads to the encoding error $\|\mathbf{Y} - \mathbf{P}^\dagger \hat{\mathbf{Y}}\|^2$. As discussed in the previous section, this error, together with the training error in the transformed label space, is used to guide the search for a good label transform.

As discussed in (Rai, Kumar, and Iii 2012), MROTS already subsumes some recent methods for multiple-output regression, including multivariate regression with covariance estimation (MRCE) (Rothman, Levina, and Zhu 2010) and multitask relationship learning (MTRL) (Zhang and Yeung 2010). Hence, the proposed model is even more general.

Inference

Given N i.i.d. samples, let $\mathbf{X} = [\mathbf{x}^{(1)}, \dots, \mathbf{x}^{(N)}]$ be the input matrix, and $\mathbf{Y} = [\mathbf{y}^{(1)}, \dots, \mathbf{y}^{(N)}]$ the corresponding label matrix. Here, we use the superscript (i) to denote entities related to the i th sample. The posterior distribution of $\{\mathbf{Z}, \mathbf{W}, \boldsymbol{\Omega}, \{\boldsymbol{\Sigma}_j\}_{j=1}^d\}$, where $\mathbf{Z} = [\mathbf{z}_1, \dots, \mathbf{z}_n]$, can be obtained as

$$\begin{aligned} & p(\mathbf{Z}, \mathbf{W}, \boldsymbol{\Omega}, \{\boldsymbol{\Sigma}_j\}_{j=1}^d | \mathbf{X}, \mathbf{Y}, \mathbf{b}) \\ & \propto p(\mathbf{Y} | \mathbf{Z}) p(\mathbf{Z}, \mathbf{W}, \boldsymbol{\Omega}, \{\boldsymbol{\Sigma}_j\}_{j=1}^d | \mathbf{X}, \mathbf{b}) \\ & = p(\mathbf{Y} | \mathbf{Z}) p(\mathbf{Z} | \mathbf{W}, \mathbf{X}, \boldsymbol{\Omega}, \mathbf{b}) p(\mathbf{W} | \{\boldsymbol{\Sigma}_j\}_{j=1}^d) p(\boldsymbol{\Omega}) p(\{\boldsymbol{\Sigma}_j\}_{j=1}^d) \\ & = p(\boldsymbol{\Omega}) \prod_{j=1}^d p(\mathbf{W}_{(j,:)} | \boldsymbol{\Sigma}_j) p(\boldsymbol{\Sigma}_j) \\ & \quad \cdot \prod_{i=1}^N p(\mathbf{y}^{(i)} | \mathbf{z}^{(i)}) p(\mathbf{z}^{(i)} | \mathbf{x}^{(i)}, \mathbf{W}, \boldsymbol{\Omega}, \mathbf{b}). \end{aligned} \quad (11)$$

In the following, alternating maximization (Bertsekas 1999) is used, i.e., (11) is maximized w.r.t. only one variable a time with the others fixed. As will be seen, each subproblem is convex and easy to solve.

Solving \mathbf{Z} with Others Fixed The optimization subproblem is

$$\begin{aligned} \min_{\mathbf{z}} \quad & \sum_{i=1}^N \lambda_0 \|\mathbf{z}^{(i)} - \mathbf{y}^{(i)}\|^2 \\ & + (\mathbf{z}^{(i)} - \mathbf{W}^T \mathbf{x}^{(i)} - \mathbf{b})^T \boldsymbol{\Omega}^{-1} (\mathbf{z}^{(i)} - \mathbf{W}^T \mathbf{x}^{(i)} - \mathbf{b}). \end{aligned}$$

Obviously, each $\mathbf{z}^{(i)}$ can be solved independently. By setting the derivative of the objective w.r.t. $\mathbf{z}^{(i)}$ to $\mathbf{0}$, we obtain

$$\mathbf{z}^{(i)} = (\lambda_0 \mathbf{I} + \boldsymbol{\Omega}^{-1})^{-1} (\boldsymbol{\Omega}^{-1} (\mathbf{W}^T \mathbf{x}^{(i)} + \mathbf{b}) + \lambda_0 \mathbf{y}^{(i)}).$$

²In (Rai, Kumar, and Iii 2012), the prior on \mathbf{W} is defined as $p(\mathbf{W}) \propto \prod_{i=1}^m \mathcal{N}(\mathbf{w}_i | \mathbf{0}, \mathbf{I}) \mathcal{MN}_{d,m}(\mathbf{W} | \mathbf{0}, \mathbf{I} \otimes \boldsymbol{\Sigma})$. As shown in their derivation, this leads to a $\text{tr}(\mathbf{W}(\boldsymbol{\Sigma}^{-1} + \mathbf{I})\mathbf{W}^T)$ term in the negative log-posterior. Hence, the effect of $\mathcal{N}(\mathbf{w}_i | \mathbf{0}, \mathbf{I})$ in $p(\mathbf{W})$ is to simply add an \mathbf{I} to $\boldsymbol{\Sigma}^{-1}$. This can be compensated in our model by adjusting the regularization parameter β_1 in (9).

Solving \mathbf{W} and \mathbf{b} with Others Fixed The optimization subproblem is

$$\min_{\mathbf{W}, \mathbf{b}} \text{tr}(\mathbf{Z} - \mathbf{W}^T \mathbf{X} - \mathbf{b} \mathbf{1}^T)^T \Omega^{-1} (\mathbf{Z} - \mathbf{W}^T \mathbf{X} - \mathbf{b} \mathbf{1}^T) + \sum_{j=1}^d \mathbf{W}_{(j,:)} \Sigma_j^{-1} \mathbf{W}_{(j,:)}^T. \quad (12)$$

On setting the derivative of \mathbf{W} to $\mathbf{0}$, we obtain its closed-form solution as

$$\text{vec}(\mathbf{W}) = \left(\Omega^{-1} \otimes (\mathbf{X} \mathbf{X}^T) + \sum_{j=1}^d \Sigma_j^{-1} \otimes \mathbf{E}_j \right)^{-1} \text{vec}(\mathbf{C}), \quad (13)$$

where $\mathbf{C} = \mathbf{X}(\mathbf{Z} - \mathbf{b} \mathbf{1}^T) \Omega^{-1}$. For \mathbf{b} , on setting its derivative to $\mathbf{0}$, we obtain

$$\mathbf{b} = \frac{1}{N} (\mathbf{Z} - \mathbf{W}^T \mathbf{X}) \mathbf{1}. \quad (14)$$

Solving Ω^{-1} with Others Fixed With the prior in (6), the optimization subproblem is

$$\min_{\Omega^{-1}} \text{tr}(\mathbf{Z} - \mathbf{W}^T \mathbf{X} - \mathbf{b} \mathbf{1}^T)^T \Omega^{-1} (\mathbf{Z} - \mathbf{W}^T \mathbf{X} - \mathbf{b} \mathbf{1}^T) - N \log |\Omega^{-1}| + \lambda_1 \text{tr}(\Omega^{-1}) + \lambda_2 \|\Omega^{-1}\|_1.$$

Ω^{-1} can be solved using standard sparse inverse covariance estimation algorithms, such as the graphical Lasso in (Friedman, Hastie, and Tibshirani 2008).

Solving Σ_j^{-1} 's with Others Fixed With the prior in (9), the optimization subproblem for each Σ_j is

$$\min_{\Sigma_j^{-1}} \mathbf{W}_{(j,:)} \Sigma_j^{-1} \mathbf{W}_{(j,:)}^T - \log |\Sigma_j^{-1}| + \beta_1 \text{tr}(\Sigma_j^{-1}) + \beta_2 \|\Sigma_j^{-1}\|_1. \quad (15)$$

Again, Σ_j^{-1} can be obtained by sparse inverse covariance estimation.

Handling Missing Labels

As discussed in the introduction, the label vectors may have missing entries. Assume that sample $\mathbf{x}^{(i)}$ has l_i observed labels and $u_i = m - l_i$ missing labels. We reorder $\mathbf{y}^{(i)}$ (and, similarly, $\mathbf{z}^{(i)}$) as $[(\mathbf{y}_l^{(i)})^T, (\mathbf{y}_u^{(i)})^T]^T$ (where $\mathbf{y}_l^{(i)} \in \mathbb{R}^{l_i}$, and $\mathbf{y}_u^{(i)} \in \mathbb{R}^{u_i}$). Similarly, for each i , we reorder Ω^{-1} by putting the l_i rows/columns corresponding to the observed labels first as $\begin{bmatrix} \mathbf{U}_i & \mathbf{V}_i \\ \mathbf{V}_i^T & \mathbf{Q}_i \end{bmatrix}$, where $\mathbf{U}_i \in \mathbb{R}^{l_i \times l_i}$, $\mathbf{V}_i \in \mathbb{R}^{l_i \times u_i}$ and $\mathbf{Q}_i \in \mathbb{R}^{u_i \times u_i}$.

Instead of estimating the values for the missing labels as in (Bucak, Jin, and Jain 2011; Chen, Zheng, and Weinberger 2013), we directly derive the posterior w.r.t. the observed labels. Analogous to (11), we have

$$\begin{aligned} & p(\{\mathbf{z}_l^{(i)}\}_{i=1}^N, \mathbf{W}, \Omega, \{\Sigma_j\}_{j=1}^d | \mathbf{X}, \{\mathbf{y}_l^{(i)}\}_{i=1}^N, \mathbf{b}) \\ & \propto p(\Omega) \prod_{j=1}^d p(\mathbf{W}_{(j,:)} | \Sigma_j) p(\Sigma_j) \\ & \cdot \prod_{i=1}^N p(\mathbf{y}_l^{(i)} | \mathbf{z}_l^{(i)}) p(\mathbf{z}_l^{(i)} | \mathbf{x}^{(i)}, \mathbf{W}, \Omega, \mathbf{b}). \end{aligned} \quad (16)$$

Note that $p(\mathbf{y}_l^{(i)} | \mathbf{z}_l^{(i)}) = \prod_{j \in l_i} p(\mathbf{y}_j^{(i)} | \mathbf{z}_j^{(i)})$ and so can be easily obtained as in $p(\mathbf{y}^{(i)} | \mathbf{z}^{(i)})$. However, this is not the case for

$p(\mathbf{z}_l^{(i)} | \mathbf{x}^{(i)}, \mathbf{W}, \Omega, \mathbf{b})$. Instead, we marginalize the missing elements from $p(\mathbf{z}^{(i)} | \mathbf{W}, \mathbf{x}^{(i)}, \Omega, \mathbf{b})$, as

$$\begin{aligned} & p(\mathbf{z}_l^{(i)} | \mathbf{W}, \mathbf{x}^{(i)}, \Omega, \mathbf{b}) \\ & = \int p([\mathbf{z}_l^{(i)T}, (\mathbf{z}_u^{(i)})^T]^T | \mathbf{W}, \mathbf{b}, \mathbf{x}^{(i)}, \Omega) d\mathbf{z}_u^{(i)}. \end{aligned} \quad (17)$$

From (Bishop 2006), this is still normally distributed, as

$$\mathbf{z}_l^{(i)} | \mathbf{W}, \mathbf{x}^{(i)}, \Omega \sim \mathcal{N}(\mathbf{W}_{(:,l_i)}^T \mathbf{x}^{(i)} + \mathbf{b}_{l_i}, \tilde{\mathbf{U}}_i), \quad (18)$$

where $\tilde{\mathbf{U}}_i = \mathbf{U}_i - \mathbf{V}_i \mathbf{Q}_i^{-1} \mathbf{V}_i^T$, and $\mathbf{W}_{(:,l_i)}$ is the submatrix of \mathbf{W} with columns corresponding to the l_i observed labels. Note that each $\mathbf{z}_l^{(i)}$ is dependent on the whole Ω matrix (via $\tilde{\mathbf{U}}_i$). Thus, even in the presence of missing labels, the inference procedure can still utilize label correlation information.

As in the previous section, we will use alternating maximization to maximize the posterior in (16). Note that the optimization subproblems for Σ_j^{-1} 's are the same as before, and thus the updates remain unchanged.

Solving $\{\mathbf{z}_l^{(i)}\}_{i=1}^N$ with Others Fixed The optimization subproblem is

$$\begin{aligned} \min_{\mathbf{z}_l^{(i)}} & \sum_{i=1}^N \|\mathbf{z}_l^{(i)} - \mathbf{y}_l^{(i)}\|^2 \\ & + (\mathbf{z}_l^{(i)} - \mathbf{W}_{(:,l_i)}^T \mathbf{x}^{(i)} - \mathbf{b}_{l_i})^T \tilde{\mathbf{U}}_i \\ & \cdot (\mathbf{z}_l^{(i)} - \mathbf{W}_{(:,l_i)}^T \mathbf{x}^{(i)} - \mathbf{b}_{l_i}). \end{aligned}$$

Setting the derivative w.r.t. each $\mathbf{z}_l^{(i)}$ to $\mathbf{0}$, we have

$$\mathbf{z}_l^{(i)} = \mathbf{W}_{(:,l_i)}^T \mathbf{x}^{(i)} + \mathbf{b}_{l_i} - \tilde{\mathbf{U}}_i^{-1} \mathbf{y}_l^{(i)}.$$

Solving \mathbf{W} and \mathbf{b} with Others Fixed The optimization subproblem is

$$\begin{aligned} \min_{\mathbf{W}, \mathbf{b}} & \sum_{i=1}^N (\mathbf{z}_l^{(i)} - \mathbf{W}_{(:,l_i)}^T \mathbf{x}^{(i)} - \mathbf{b}_{l_i})^T \tilde{\mathbf{U}}_i (\mathbf{z}_l^{(i)} - \mathbf{W}_{(:,l_i)}^T \mathbf{x}^{(i)} - \mathbf{b}_{l_i}) \\ & + \sum_{j=1}^d \mathbf{W}_{(j,:)} \Sigma_j^{-1} \mathbf{W}_{(j,:)}^T. \end{aligned} \quad (19)$$

Unlike (12), a closed-form solution cannot be obtained for this convex problem. Thus, we optimize \mathbf{W} by gradient descent. As for \mathbf{b} , we have the closed-form solution

$$\mathbf{b} = \left(\sum_{i=1}^N \Xi_i(\tilde{\mathbf{U}}_i) \right)^{-1} \sum_{i=1}^N \Xi_i \left(\tilde{\mathbf{U}}_i (\mathbf{z}_l^{(i)} - \mathbf{W}_{(:,l_i)}^T \mathbf{x}^{(i)}) \right),$$

where Ξ_i is an operator that ‘‘expands’’ a matrix $\mathbf{A} \in \mathbb{R}^{l_i \times l_i}$ into $\begin{bmatrix} \mathbf{A} & \mathbf{0} \\ \mathbf{0} & \mathbf{0} \end{bmatrix} \in \mathbb{R}^{m \times m}$.

Solving Ω^{-1} with Others Fixed The optimization subproblem is

$$\begin{aligned} \min_{\Omega^{-1}} & \sum_{i=1}^N (\mathbf{y}_l^{(i)} - \mathbf{W}_{(:,l_i)}^T \mathbf{x}^{(i)} - \mathbf{b}_{l_i})^T \tilde{\mathbf{U}}_i (\mathbf{y}_l^{(i)} - \mathbf{W}_{(:,l_i)}^T \mathbf{x}^{(i)} - \mathbf{b}_{l_i}) \\ & - \ln |\tilde{\mathbf{U}}_i| + \lambda_1 \text{tr}(\Omega^{-1}) + \lambda_2 \|\Omega^{-1}\|_1. \end{aligned}$$

This can be solved by iterative soft thresholding (Beck and Teboulle 2009). Specifically, we decompose the objective into two parts, as:

$$f(\Omega) = \left(\mathbf{y}_l^{(i)} - \mathbf{W}_{(:,l_i)}^T \mathbf{x}^{(i)} - \mathbf{b}_{l_i} \right)^T \tilde{\mathbf{U}}_i \left(\mathbf{y}_l^{(i)} - \mathbf{W}_{(:,l_i)}^T \mathbf{x}^{(i)} - \mathbf{b}_{l_i} \right) - \ln |\tilde{\mathbf{U}}_i| + \lambda_1 \text{tr}(\Omega^{-1}),$$

$$g(\Omega) = \lambda_2 \|\Omega^{-1}\|_1.$$

Since Ω is positive semidefinite (psd), instead of performing projected gradient descent (which requires the potentially expensive projection onto the psd cone in every iteration), we update Ω^{-1} based on its factorization. In each iteration,

1. We factorize Ω^{-1} as $\mathbf{G}\mathbf{G}^T$, and perform a one-step gradient descent of $f(\Omega)$ on \mathbf{G} ;
2. recompute Ω^{-1} from the updated \mathbf{G} ;
3. sparsify Ω^{-1} by shrinking each of its elements as $(|(\Omega^{-1})_{ij}| - \tau)_+ \text{sign}((\Omega^{-1})_{ij})$, where $\tau = \lambda_2 \eta$, η is the stepsize for gradient descent, and $(a)_+ = \max\{a, 0\}$.

Experiments

Setup

In this section, experiments are performed on five image annotation data sets³ (Table 1) used in (Guillaumin et al. 2009). For each image, 1000 SIFT features are extracted.

Table 1: Data sets used.

data set	#labels	#samples	avg #positive labels per sample	max #negative labels per sample
pascal07	20	9,963	1.5	6
mirflickr	38	25,000	4.7	17
corel5k	260	4,999	3.4	5
espgame	268	23,641	4.7	15
iaprtc12	291	19,627	5.7	23

The proposed method, called “multilabel classification with label correlations and missing labels” (LCML), is compared with the following methods:

1. Multiple-output regression with output and task structures (MROTS) (Rai, Kumar, and Iii 2012): It leverages both the task structure on \mathbf{W} and output structure on \mathbf{Y} . However, MROTS assumes the Σ_i 's for all features are the same. Moreover, it is for regression problems and does not consider rounding its output to a binary prediction.
2. Conditional principal label space transformation (CPLST) (Chen and Lin 2012);
3. Max-margin multilabel classifier (M3L)⁴ (Hariharan et al. 2010);
4. Multilabel ranking with group lasso (MLRGL)⁵ (Bucak, Jin, and Jain 2011);
5. Fast image tagging (FastTag)⁶ (Chen, Zheng, and Weinberger 2013);

³<http://lear.inrialpes.fr/people/guillaumin/data.php>

⁴Code is from <http://www.cs.berkeley.edu/~bharath2/codes/M3L/download.html>

⁵Code is from <http://www.cse.msu.edu/~bucakser/software.html>

⁶Code is from <http://www.cse.wustl.edu/~mchen/>

6. Classifier chain (CC) (Read et al. 2009);

7. Binary relevance (BR) (Tsoumakos and Katakis 2007): It serves as a baseline that trains each label independently.

As the transformed labels in CPLST are real-valued, we use ridge regression as its base learner. For consistency, it is also used for CC and BR. Parameter tuning for all the methods is based on a validation set obtained by randomly sampling 30% of the training data. Moreover, some of the above methods (such as MROTS, CPLST, CC and BR) rely on a threshold to decide how many labels are to be predicted for each sample. However, this threshold setting depends heavily on the application. As in (Guillaumin et al. 2009), we avoid this problem by predicting as positive the five labels with the largest prediction scores. Performance is then evaluated by

$$\text{macro-F1} = \frac{1}{m} \sum_{j=1}^m \frac{2 \sum_{i=1}^N \hat{y}_j^{(i)} y_j^{(i)}}{\sum_{i=1}^N \hat{y}_j^{(i)} + \sum_{i=1}^N y_j^{(i)}},$$

$$\text{micro-F1} = \frac{1}{N} \sum_{i=1}^N \frac{2 \sum_{j=1}^m \hat{y}_j^{(i)} y_j^{(i)}}{\sum_{j=1}^m \hat{y}_j^{(i)} + \sum_{j=1}^m y_j^{(i)}},$$

which are commonly used in multilabel classification (Read et al. 2009; Petterson and Caetano 2011; Tai and Lin 2012). The higher the F1 value, the better the performance.

Performance Comparison

Results based on 5-fold cross-validation are shown in Table 2. As can be seen, LCML performs significantly better than the others on all data sets. Note that M3L and CC are even outperformed by BR. For M3L, this may be due to that the provided label correlations are too crude. This has also been noted in (Hariharan et al. 2010) that different label priors can greatly affect the performance. For CC, it is also known that the chain's order is important. Read et al. (2009) recommended the use of an ensemble of CC, but this can be very expensive. Thus, the label correlations, if inaccurately specified, may hurt performance.

Experiments on Data Sets with Missing Labels

We generate the missing labels as follows. Recall that there are m labels. For each training sample, we choose half of them as observed and the rest as missing. However, as each sample typically has very few positive labels, a random label splitting is likely to result in only negative labels being observed. Thus, for each sample, we make sure that there are $k = 1, 2, 3$ positive observed labels (if the sample have fewer than k positive labels, all its positive labels are selected). We compare LCML with MLRGL and FastTag, which are also capable of handling missing labels.⁷ BR is also included as a baseline. In each binary label classification task, it simply removes samples with labels.

Table 3 shows the results based on 5-fold cross-validation. As can be seen, LCML still significantly outperforms the others (except for $k = 2$ on mirflickr). Moreover, the performance does not always improve with k , as the number of missing labels is much larger than the maximum value of k . Nevertheless, even for $k = 1$, the F1 values obtained by LCML are very close to those obtained on the complete labels in Table 2. On corel5k, LCML even performs better when labels are missing. One possible reason is that with complete labels, we need to learn the $m \times n$ label matrix \mathbf{Z} . When labels are missing, they are integrated out in (17) and only the submatrix of \mathbf{Z} corresponding to the observed labels needs to be learned. Thus, the number of free parameters is reduced,

⁷Recall that MLRGL and FastTag assume the missing labels are negative.

Table 2: Results on data sets with complete labels. The best and comparable results (according to the pairwise t-test with 95% confidence) are highlighted.

macro-F1								
data set	LCML	MROTS	CPLST	M3L	MLRGL	FastTag	CC	BR
pascal07	0.3591 ± 0.0055	0.3587 ± 0.0061	0.3268 ± 0.0055	0.1539 ± 0.0641	0.3486 ± 0.0075	0.2942 ± 0.0133	0.2037 ± 0.0051	0.3267 ± 0.0055
mirflickr	0.4992 ± 0.0052	0.4928 ± 0.0043	0.4930 ± 0.0046	0.2418 ± 0.0025	0.4958 ± 0.0078	0.4681 ± 0.0057	0.2479 ± 0.0032	0.4930 ± 0.0046
corel5k	0.2077 ± 0.0562	0.2046 ± 0.0571	0.2005 ± 0.0493	0.0084 ± 0.0012	0.1321 ± 0.0443	0.2038 ± 0.0378	0.0223 ± 0.0071	0.2005 ± 0.0493
espgame	0.2380 ± 0.0130	0.2312 ± 0.0164	0.2328 ± 0.0167	0.0153 ± 0.0100	0.1254 ± 0.0076	0.2287 ± 0.0150	0.0455 ± 0.0070	0.2328 ± 0.0167
iaprtc12	0.2463 ± 0.0409	0.2455 ± 0.0469	0.2376 ± 0.0429	0.0276 ± 0.0074	0.1273 ± 0.0407	0.2285 ± 0.0423	0.0275 ± 0.0041	0.2377 ± 0.0429
micro-F1								
data set	LCML	MROTS	CPLST	M3L	MLRGL	FastTag	CC	BR
pascal07	0.3493 ± 0.0050	0.3489 ± 0.0054	0.3181 ± 0.0051	0.1481 ± 0.0603	0.3386 ± 0.0067	0.2813 ± 0.0141	0.2039 ± 0.0052	0.3181 ± 0.0051
mirflickr	0.4665 ± 0.0043	0.4605 ± 0.0053	0.4608 ± 0.0055	0.2131 ± 0.0029	0.4668 ± 0.0096	0.4365 ± 0.0068	0.2476 ± 0.0030	0.4608 ± 0.0055
corel5k	0.2071 ± 0.0554	0.2038 ± 0.0559	0.1980 ± 0.0484	0.0081 ± 0.0012	0.1303 ± 0.0434	0.2012 ± 0.0367	0.0220 ± 0.0070	0.1980 ± 0.0484
espgame	0.2273 ± 0.0141	0.2203 ± 0.0181	0.2219 ± 0.0183	0.0146 ± 0.0090	0.1185 ± 0.0008	0.2179 ± 0.0169	0.0448 ± 0.0070	0.2219 ± 0.0183
iaprtc12	0.2405 ± 0.0453	0.2397 ± 0.0474	0.2304 ± 0.0433	0.0259 ± 0.0068	0.1244 ± 0.0413	0.2209 ± 0.0432	0.0280 ± 0.0036	0.2305 ± 0.0433

though (17) depends on the quality of the estimated distribution $p([\mathbf{z}_l^{(i)T}, (\mathbf{z}_u^{(i)T})^T | \mathbf{W}, \mathbf{x}^{(i)}, \boldsymbol{\Omega})$ and may introduce error. The final performance thus depends on which factor is more important.

Conclusion

In this paper, we proposed a probabilistic model for multilabel classification. While inspired by the label transformation approach, the model is expressed in the original label space instead of the transformed label space. This allows flexibility in the handling of both label dependencies and missing labels, while still maintaining a simple inference procedure. Experimental results on data sets with both complete and missing labels demonstrate that the proposed algorithm can consistently outperform the state-of-the-art.

Acknowledgment

This research was supported in part by the Research Grants Council of the Hong Kong Special Administrative Region (Grant 614012).

References

- Beck, A., and Teboulle, M. 2009. A fast iterative shrinkage-thresholding algorithm for linear inverse problems. *SIAM Journal on Imaging Sciences* 2(1):183–202.
- Bertsekas, D. P. 1999. *Nonlinear Programming*. Athena Scientific.
- Bishop, C. M. 2006. *Pattern Recognition and Machine Learning*. Springer-Verlag.
- Bucak, S.; Jin, R.; and Jain, A. 2011. Multi-label learning with incomplete class assignments. In *Proceedings of the IEEE Conference on Computer Vision and Pattern Recognition*, 2801–2808.
- Chen, Y.-N., and Lin, H.-T. 2012. Feature-aware label space dimension reduction for multi-label classification. In *Advances in Neural Information Processing Systems 25*, 1538–1546.
- Chen, M.; Zheng, A.; and Weinberger, K. Q. 2013. Fast image tagging. In *Proceedings of the 30th International Conference on Machine Learning*, 1274–1282.
- Duygulu, P.; Barnard, K.; Freitas, N.; and Forsyth, D. 2002. Object recognition as machine translation: Learning a lexicon for a fixed image vocabulary. In *Proceedings of the 7th European Conference on Computer Vision*, 97–112.
- Friedman, J.; Hastie, T.; and Tibshirani, R. 2008. Sparse inverse covariance estimation with the graphical lasso. *Biostatistics* 9(3):432–441.
- Goldberg, A. B.; Zhu, X.; Recht, B.; Xu, J.-M.; and Nowak, R. 2010. Transduction with matrix completion: Three birds with one

Table 3: Results on data sets with 50% missing labels and k positive observed labels.

macro-F1 ($k = 1$)				
data set	LCML	MLRGL	FastTag	BR
pascal07	0.3480 ± 0.0069	0.3451 ± 0.0080	0.2491 ± 0.0115	0.3050 ± 0.0054
mirflickr	0.4670 ± 0.0019	0.4579 ± 0.0093	0.4601 ± 0.0112	0.4549 ± 0.0024
corel5k	0.2403 ± 0.0544	0.1100 ± 0.0156	0.1998 ± 0.0107	0.1417 ± 0.0281
espgame	0.2327 ± 0.0196	0.1462 ± 0.0118	0.1790 ± 0.0082	0.1936 ± 0.0146
iaprtc12	0.2362 ± 0.0458	0.0599 ± 0.0393	0.1920 ± 0.0051	0.2097 ± 0.0345
micro-F1 ($k = 1$)				
data set	LCML	MLRGL	FastTag	BR
pascal07	0.3396 ± 0.0064	0.3363 ± 0.0074	0.2455 ± 0.0108	0.2981 ± 0.0050
mirflickr	0.4453 ± 0.0032	0.4393 ± 0.0083	0.4170 ± 0.0118	0.4320 ± 0.0039
corel5k	0.2375 ± 0.0536	0.1087 ± 0.0163	0.1950 ± 0.0108	0.1403 ± 0.0275
espgame	0.2235 ± 0.0212	0.1401 ± 0.0118	0.1701 ± 0.0080	0.1858 ± 0.0157
iaprtc12	0.2312 ± 0.0451	0.0587 ± 0.0383	0.1901 ± 0.0050	0.2053 ± 0.0345
macro-F1 ($k = 2$)				
data set	LCML	MLRGL	FastTag	BR
pascal07	0.3509 ± 0.0057	0.3451 ± 0.0080	0.2484 ± 0.0146	0.2806 ± 0.0065
mirflickr	0.4537 ± 0.0077	0.4579 ± 0.0093	0.4352 ± 0.0500	0.4442 ± 0.0043
corel5k	0.2407 ± 0.0503	0.1100 ± 0.0156	0.1808 ± 0.0109	0.0180 ± 0.0101
espgame	0.2302 ± 0.0203	0.1462 ± 0.0115	0.2222 ± 0.0045	0.1842 ± 0.0131
iaprtc12	0.2355 ± 0.0451	0.0599 ± 0.0393	0.1800 ± 0.0071	0.1976 ± 0.0325
micro-F1 ($k = 2$)				
data set	LCML	MLRGL	FastTag	BR
pascal07	0.3426 ± 0.0053	0.3363 ± 0.0074	0.2449 ± 0.0137	0.2739 ± 0.0058
mirflickr	0.4367 ± 0.0076	0.4393 ± 0.0083	0.4156 ± 0.0471	0.4208 ± 0.0051
corel5k	0.2380 ± 0.0495	0.1087 ± 0.0163	0.1746 ± 0.0110	0.0176 ± 0.0098
espgame	0.2212 ± 0.0220	0.1400 ± 0.0118	0.2130 ± 0.0044	0.1769 ± 0.0145
iaprtc12	0.2309 ± 0.0444	0.0587 ± 0.0383	0.1712 ± 0.0071	0.1934 ± 0.0326
macro-F1 ($k = 3$)				
data set	LCML	MLRGL	FastTag	BR
pascal07	0.3501 ± 0.0063	0.3451 ± 0.0080	0.2437 ± 0.0061	0.1436 ± 0.0083
mirflickr	0.4613 ± 0.0030	0.4579 ± 0.0093	0.4552 ± 0.0192	0.4128 ± 0.0021
corel5k	0.2397 ± 0.0534	0.1100 ± 0.0156	0.1808 ± 0.0080	0.0268 ± 0.0169
espgame	0.2228 ± 0.0240	0.1462 ± 0.0115	0.2150 ± 0.0084	0.1613 ± 0.0113
iaprtc12	0.2300 ± 0.0370	0.0599 ± 0.0393	0.1852 ± 0.0060	0.1659 ± 0.0241
micro-F1 ($k = 3$)				
data set	LCML	MLRGL	FastTag	BR
pascal07	0.3418 ± 0.0058	0.3363 ± 0.0074	0.2404 ± 0.0055	0.1397 ± 0.0076
mirflickr	0.4440 ± 0.0039	0.4393 ± 0.0083	0.4156 ± 0.0166	0.3895 ± 0.0030
corel5k	0.2371 ± 0.0526	0.1087 ± 0.0163	0.1746 ± 0.0080	0.0263 ± 0.0166
espgame	0.2143 ± 0.0256	0.1400 ± 0.0118	0.2047 ± 0.0079	0.1551 ± 0.0126
iaprtc12	0.2258 ± 0.0382	0.0587 ± 0.0383	0.1770 ± 0.0059	0.1623 ± 0.0242

- stone. In *Advances in Neural Information Processing Systems*, 757–765.
- Guillaumin, M.; Mensink, T.; Verbeek, J.; and Schmid, C. 2009. Tagprop: Discriminative metric learning in nearest neighbor models for image auto-annotation. In *Proceedings of the International Conference on Computer Vision*, 309–316.
- Gupta, A., and Nagar, D. 2000. *Matrix Variate Distributions*. Chapman & Hall/CRC.
- Hariharan, B.; Zelnik-Manor, L.; Vishwanathan, S.; and Varma, M. 2010. Large scale max-margin multi-label classification with priors. In *Proceedings of the 27th International Conference on Machine Learning*, 423–430.
- Hsu, D.; Kakade, S.; Langford, J.; and Zhang, T. 2009. Multi-label prediction via compressed sensing. In *Advances in Neural Information Processing Systems 22*, 772–780.
- Kapoor, A.; Viswanathan, R.; and Jain, P. 2012. Multilabel classification using bayesian compressed sensing. In *Advances in Neural Information Processing Systems*, 2654–2662.
- Koivisto, M., and Sood, K. 2004. Exact Bayesian structure discovery in Bayesian networks. *Journal of Machine Learning Research* 5:549–573.
- Lauritzen, S. L. 1996. *Graphical Models*. Oxford University Press.
- Petterson, J., and Caetano, T. 2011. Submodular multi-label learning. *Advances in Neural Information Processing Systems 24*.
- Rai, P.; Kumar, A.; and Iii, H. D. 2012. Simultaneously leveraging output and task structures for multiple-output regression. In *Advances in Neural Information Processing Systems 25*, 3194–3202.
- Read, J.; Pfahringer, B.; Holmes, G.; and Frank, E. 2009. Classifier chains for multi-label classification. In *Proceedings of the European Conference on Machine Learning*, 254–269.
- Rothman, A. J.; Levina, E.; and Zhu, J. 2010. Sparse multivariate regression with covariance estimation. *Journal of Computational and Graphical Statistics* 19(4):947–962.
- Tai, F., and Lin, H. 2012. Multilabel classification with principal label space transformation. *Neural Computation* 24(9):2508–2542.
- Tsoumakas, G., and Katakis, I. 2007. Multi-label classification: An overview. *International Journal of Data Warehousing and Mining* 3:1–13.
- Tsoumakas, G.; Katakis, I.; and Vlahavas, I. 2010. Mining multi-label data. In Maimon, O., and Rokach, L., eds., *Data Mining and Knowledge Discovery Handbook*. Springer. 667–685.
- Von Ahn, L., and Dabbish, L. 2004. Labeling images with a computer game. In *Proceedings of the SIGCHI Conference on Human Factors in Computing Systems*, 319–326.
- Xu, M.; Jin, R.; and Zhou, Z.-H. 2013. Speedup matrix completion with side information: Application to multi-label learning. In *Advances in Neural Information Processing Systems*, 2301–2309.
- Yu, H.-F.; Jain, P.; and Dhillon, I. S. 2014. Large-scale multi-label learning with missing labels. In *Proceedings of the 31th International Conference on Machine Learning*, 593–601.
- Yuan, M., and Lin, Y. 2006. Model selection and estimation in regression with grouped variables. *Journal of the Royal Statistical Society, Series B* 68(1):49–67.
- Zhang, Y., and Yeung, D.-Y. 2010. A convex formulation for learning task relationships in multi-task learning. In *Proceedings of the 26th Conference on Uncertainty in Artificial Intelligence*, 733–742.
- Zhang, M.-L., and Zhang, K. 2010. Multi-label learning by exploiting label dependency. In *Proceedings of the 16th International Conference on Knowledge Discovery and Data Mining*, 999–1008.
- Zhang, M.-L., and Zhou, Z.-H. 2013. A review on multi-label learning algorithms. *IEEE Transactions on Knowledge and Data Engineering* 99(PrePrints):1.